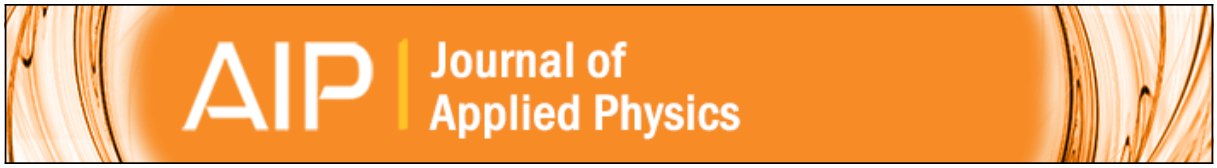


# Mn behavior in Ge 0.96 Mn 0.04 magnetic thin films grown on Si

Yong Wang, Jin Zou, Zuoming Zhao, Xinhai Han, Xiaoyu Zhou, and Kang L. Wang

Citation: Journal of Applied Physics **103**, 066104 (2008); doi: 10.1063/1.2875110

View online: http://dx.doi.org/10.1063/1.2875110

View Table of Contents: http://scitation.aip.org/content/aip/journal/jap/103/6?ver=pdfcov

Published by the AIP Publishing



# Mn behavior in $Ge_{0.96}Mn_{0.04}$ magnetic thin films grown on Si

Yong Wang,[1] Jin Zou,[1,a)] Zuoming Zhao,[2] Xinhai Han,[2] Xiaoyu Zhou,[2] and Kang L. Wang[2]
[1]*School of Engineering and Centre for Microscopy and Microanalysis, The University of Queensland, Brisbane QLD 4072, Australia*
[2]*Device Research Lab, Electrical Engineering, University of California at Los Angeles, Los Angeles, California 90095, USA*

(Received 18 December 2007; accepted 20 December 2007; published online 18 March 2008)

Mn behaviors in the $Ge_{0.96}Mn_{0.04}$ thin films grown on Si (001) substrates by molecular beam epitaxy were investigated by high resolution transmission electron microscopy, electron energy loss spectroscopy, and energy dispersive spectroscopy. Unlike the previously reported case of GeMn thin films grown on Ge, Mn has been found to be diffused toward to the surface during the thin film growth. When the Mn concentration is sufficiently high, $Mn_5Ge_3$ clusters may be formed. Further annealing of the high Mn concentrated thin film promotes the formation of $\alpha$-Mn metallic clusters. We believe that all these extraordinary phenomena are attributed to Si as the substrate. © *2008 American Institute of Physics*. [DOI: 10.1063/1.2875110]

Since the growth of GeMn diluted magnetic semiconductor (DMS) was reported in early 2000s,[1] extensive attention has been paid in terms of its promising applications in spintronic devices.[2–10] One of the key issues to achieve GeMn DMS is to uniformly dope Mn into the Ge matrix.[7,10] It has been reported that the Mn dilution in Ge depends strongly upon the substrate temperature and that inhomogeneous Mn distributed in the Ge films tends to the formation of Mn-rich precipitates, such as $Mn_5Ge_3$[4–6] and $Mn_{11}Ge_8$[8,9] phases, which makes it complicated to understand the origin of ferromagnetism of GeMn DMS films. Most of the previous studies have been focused on the structural and magnetic properties of these Mn-rich clusters in GeMn films grown on Ge substrates. However, little attention has been paid on the Mn behavior in the GeMn films grown on Si substrates, although such information is of great significance, both scientifically and technologically.

In this letter, through detailed transmission electron microscopy (TEM), electron energy loss spectroscopy (EELS) and energy dispersive spectroscopy (EDS) investigations, the Mn behavior in $Ge_{0.96}Mn_{0.04}$ thin films grown on Si (001) substrates with different film thicknesses and the annealing effect on the Mn behaviors are comprehensively investigated. The fundamental reasons behind the observed new physical phenomenon are discussed.

Two $Ge_{0.96}Mn_{0.04}$ thin films were grown on Si (001) substrates by a Perkin-Elmer solid source molecular beam epitaxy with nominal thicknesses of 15 nm (sample A) and 80 nm (sample B). The Si substrates were cleaned by $H_2SO_4$:$H_2O_2$ (5:3) and 10% HF with a final step of HF etching. Native oxide was removed by 800 °C annealing for 10 min in vacuum. After that, 4% Mn-doped Ge was deposited with a growth rate of 0.02 nm/s on Si (001) substrates at 250 °C. Half of the two samples were further annealed at 400 °C for 30 min in vacuum. All as-grown and annealed samples were characterized by x-ray diffraction (XRD), cross-sectional TEM. TEM specimens were prepared using a tripod technique, followed by a final ion beam thinning. The TEM and EELS experiments were performed in a FEI Tecnai F30 TEM equipped with a Gatan image filtering system and the EDS examinations were carried out in a FEI Tecnai F20 TEM.

Figures 1(a) and 1(b) are typical cross-sectional TEM images of the as-grown and annealed samples A and show their general morphology of the GeMn thin films. From these figures, a relative uniform crystalline layer, adjacent to the Si substrates and topped with an amorphous layer, can be revealed in both cases. It can be noted that the thickness of the amorphous layer (~2.5 nm) in the annealed case is thinner than that (~5 nm) in the as-grown case, indicating that partial crystallization has been taken place during the annealing. In fact, this conclusion can be further supported by the thick-

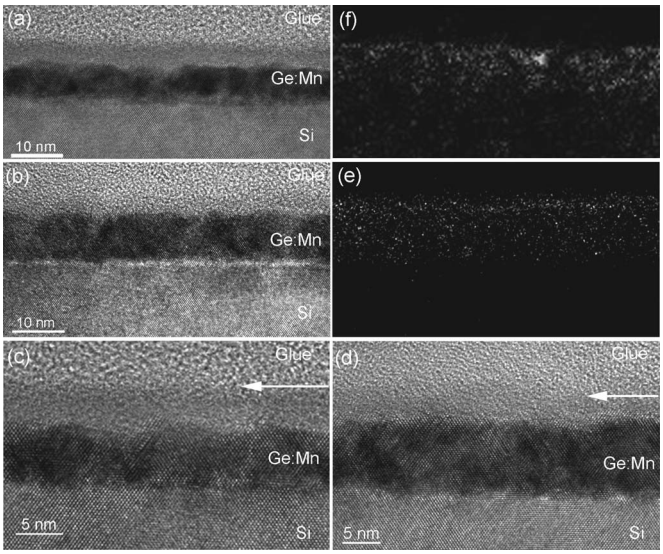


FIG. 1. Typical TEM images of the as-grown (a) and the annealed (b) samples A; (c) and (d) are the corresponding HRTEM images of as-grown and annealed samples A, respectively; (e) and (f) EFTEM Mn elemental maps of corresponds to regions given by (a) and (b), respectively.

a)Electronic mail: j.zou@uq.edu.au.

 

ened crystalline layer in the annealed case. To understand the structural variation of the two cases, high resolution TEM (HRTEM) was carried out and typical ⟨110⟩ zone-axis HRTEM images are, respectively, shown on Figs. 1(c) and 1(d) for the two cases, where amorphous layers can be clearly seen. From these HRTEM images, stacking faults in the crystalline layers can be seen for both cases. No structural clusters were found in sample A through our extensive HRTEM investigations and no secondary phases were detected by our XRD measurements (not shown here). To further understand Mn distribution in the GeMn film (crystalline and amorphous), energy filtered TEM (EFTEM) was preformed.[11] Figures 1(e) and 1(f) are the EFTEM Mn elemental maps that correspond to Figs. 1(b) and 1(a), respectively. It is of interest to note that, in the as-grown case, a higher Mn concentration is found in the amorphous layer [when comparing Figs. 1(a) and 1(f)]. It should be noted that the overall concentration of Mn is low, so that the contrast in the Mn maps tends to be faint. Nevertheless, the distribution of Mn in the entire film can be clearly seen. In contrast, the Mn map in the annealed case shows some Mn distribution in the entire film, suggesting that the annealing has not only promoted crystallization, but also promoted the redistribution of Mn within the entire GeMn film. Nevertheless, a higher Mn concentration can still be observed in the surface region in the annealed sample [refer to Fig. 1(e)]. The fact that, in the case of the as-grown sample, most of Mn was found in the topmost layer suggests that, during the growth of the GeMn film, a dynamic Mn diffusion has taken place, even at a relatively low growth temperature (250 °C in our case), in which Mn diffuses towards to the top surface. An interesting physical phenomenon arises: why Mn diffuses towards to the surface during the thin film growth. To understand this, we note that the lattice parameter of Ge ($a$=0.566 nm) is larger than that of Si ($a$=0.543 nm),[12] leading to the grown Ge dominated layer ($Ge_{0.96}Mn_{0.04}$) experiencing a compressive strain from its underlying Si substrate. Since the atomic radius of Mn (0.140 nm) is larger than that of Ge (0.125 nm),[13] it is energetically favorable for Mn to be diffused away from the GeMn/Si interface to reduce the otherwise increased compressive strain. Moreover, since Mn has been found to be active in terms of their diffusion in solids,[14,15] the realization of Mn diffusion in our case is therefore expected.

For the case of thicker $Ge_{0.96}Mn_{0.04}$ thin films, Figs. 2(a) and 2(b) are, respectively, typical TEM images of the as-grown and the annealed samples B. Compared with sample A, the thickness of the GeMn films tends to be nonuniform and a thin and discontinued amorphous-like layer is seen for both as-grown and annealed samples [refer to Figs. 2(a) and 2(b)]. Figures 2(c) and 2(d) are their corresponding Mn maps, respectively. For both samples, Figs. 2(c) and 2(d) confirmed that Mn is dominated in the top surface. Since the overall Mn content in the thicker GeMn film is higher than that in the thinner film, the Mn accumulation leads to a strong Mn contrast in the EFTEM images. The careful comparison between Figs. 2(a) and 2(c) suggests that Mn-containing clusters correspond to the dark regions near the top of the crystalline layer, as one of them marked in Fig. 2(a). HRTEM investigations were carried out to determine

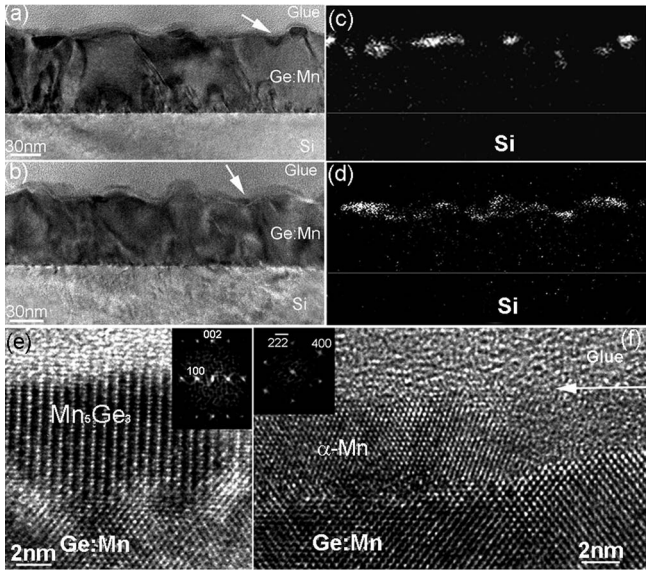


FIG. 2. (a) and (b) Typical TEM image of the as-grown and the annealed samples B, respectively; (c) and (d) are the corresponding Mn maps of (a) and (b), respectively; (e) HRTEM image of a typical $Mn_5Ge_3$ cluster epitaxially grown on the Ge(Mn) lattice showing the crystallographic orientation relationship; (f) HRTEM image of a typical $\alpha$-Mn metallic cluster epitaxially grown on the Ge(Mn) lattice showing the crystallographic orientation relationship.

the nature of Mn-rich clusters. Figure 2(e) is such an example, in which a Mn-containing cluster is clearly seen on top of the Ge lattice. Using the lattice spacing of Ge as a reference, the lattice spacings of the Mn-containing cluster can be determined as 0.62 and 0.25 nm, which are well matched with the distances of (100) and (002) atomic planes of the hexagonal $Mn_5Ge_3$ phase. The fast Fourier transformation (FFT—equivalent to electron diffraction[16]) was also performed to further confirm its crystal structure and the result is shown in the inset of Fig. 2(e). Both the HRTEM image and its corresponding FFT pattern indicate the cluster belongs to the hexagonal $Mn_5Ge_3$ phase,[12,17] and the crystallographic relationship between the $Mn_5Ge_3$ cluster and the $Ge_{0.96}Mn_{0.04}$ (GeMn) matrix can be determined as $[001]_{Mn_5Ge_3}\|[001]_{GeMn}$ and $[010]_{Mn_5Ge_3}\|[1\bar{1}0]_{GeMn}$, which is consistent with the result previously reported.[4] Our extensive HRTEM investigations suggest no other Mn-containing phases in the as-grown GeMn films.

Interestingly, in the annealed sample B, both the $\alpha$-Mn clusters with the lattice parameter of $a$=0.89 nm (Ref. 15) and $Mn_5Ge_3$ clusters can be constantly observed on the top region of the GeMn films. A typical example of the $\alpha$-Mn nanoparticles [arrowed in Fig. 2(b)] is shown in Fig. 2(f), in which the $\alpha$-Mn cluster is epitaxially grown on the underlying GeMn film. From the FFT pattern [the inset in Fig. 2(f)], the crystallographic relationship between the $\alpha$-Mn cluster and the GeMn film can be determined as $[1\bar{1}\bar{1}]_{\alpha\text{-Mn}}\|[001]_{GeMn}$ and $[100]_{\alpha\text{-Mn}}\|[111]_{GeMn}$.

There are two physical phenomena that need to be understood: (1) why and how the $Mn_5Ge_3$ clusters were formed in the thicker GeMn film (sample B), and (2) why and how the $\alpha$-Mn clusters were formed in the thicker GeMn film (sample B). To understand the first phenomenon, we note

TABLE I. Mn concentration variation from the film surface to the interface for the four samples.

| Sample (GeMn thin film on Si substrate) | Mn concentration (%) | | | |
|---|---|---|---|---|
| | Film surface | Middle area (near surface) | Middle area (near bottom) | Interface (near Si) |
| Sample A (15 nm) | 5 | 3 | 2 | 1 |
| Annealed sample A | 4 | 4 | 3 | 2 |
| Sample B (80 nm) | 23 | 14 | 1 | 1 |
| Annealed sample B | 29 | 10 | 1 | 0 |

that (1) the diffusion of Mn is very active and is significantly dependent on the temperature;[14,15] (2) Mn tends to diffuse to the surface during the growth as discussed earlier; (3) the overall Mn concentration in the thicker GeMn film is higher than that in the thinner film; and (4) there is a negative adhesive energy (−0.0717 eV/atom) for the $Mn_5Ge_3$ phase, which is favorable for the formation of the compound.[18] As a consequence, $Mn_5Ge_3$ clusters may be formed when the Mn concentration and the temperature are sufficient for the nucleation and growth of the clusters. The fact that no Mn-containing clusters (such as $Mn_5Ge_3$) were observed in the annealed sample A suggests that the nucleation of Mn-containing clusters needs a threshold concentration. Below that no nucleation of Mn-containing clusters takes place, which is also consistent with the previous report.[4] To further support our argument, extensive EDS investigations under scanning TEM mode were carried out to present quantitative information in terms of the Mn distribution and the results are summarized in Table I. Significantly high Mn concentration near the surface for the thicker films is clearly demonstrated, which confirms that a large amount of Mn atoms has been diffused into the surface region. These results also imply that the postannealing is not necessary for the formation of $Mn_5Ge_3$, but enhances the Mn diffusion.

To understand the second physical phenomenon, we compare Figs. 1(b) and 2(b), in which the annealing process lead to different Mn behaviors for different GeMn thin film thicknesses. For the case of the thinner film, the enhanced Mn diffusion leads to Mn diffusion back to the GeMn film; while for the case of the thicker film, the enhanced Mn diffusion leads to the formation of $\alpha$-Mn metallic clusters near the surface. Since the thicker film provides a higher Mn concentration, the experiment results suggest the nucleation and growth of $\alpha$-Mn clusters also needs a threshold concentration. The fact that the $\alpha$-Mn clusters have been only found in the annealed thicker sample indicates that the nucleation and growth of $\alpha$-Mn clusters also needs a threshold temperature, possibly due to $\alpha$-Mn having a higher adhesive energy (~0.1486 eV/atom).[18] It should be mentioned that, for sample B, there is no significant change in the $Mn_5Ge_3$ density before and after the annealing, suggesting that the annealing results predominately in the formation of the $\alpha$-Mn clusters.

In conclusion, we have systematically examined the nature of Mn doped in GeMn films grown on Si (001) substrates. It has been found that (1) a dynamic Mn diffusion during the GeMn growth leads to a higher Mn concentration in the surface region; (2) $Mn_5Ge_3$ clusters may be formed near the surface during the film growth when a threshold Mn concentration is reached; and (3) $\alpha$-Mn metallic clusters can be formed when both the threshold Mn concentration and the threshold temperature are reached. Our results also indicate that the Si substrate has played a key role in the Mn behaviors in GeMn thin films.

The Australia Research Council, Focus Center Research Program (FCRP)—Center on Functional Engineered Nano Architectonics (FENA), and Western Institution of Nanoelctronics (WIN) are acknowledged for their financial supports to this joint project.

[1] Y. D. Park, A. T. Hanbicki, S. C. Erwin, C. S. Hellberg, J. M. Sullivan, J. E. Mattson, T. F. Ambrose, A. Wilson, G. Spanos, and B. T. Jonker, Science **295**, 651 (2002).
[2] J. S. Kang, G. Kim, S. C. Wi, S. S. Lee, S. Choi, S. Cho, S. W. Han, K. H. Kim, H. J. Song, H. J. Shin, A. Sekiyama, S. Kasai, S. Suga, and B. I. Min, Phys. Rev. Lett. **94**, 147202 (2005).
[3] Y. X. Chen, S. S. Yan, Y. Fang, Y. F. Tian, S. Q. Xiao, G. L. Liu, Y. H. Liu, and L. M. Mei, Appl. Phys. Lett. **90**, 052508 (2007).
[4] C. Bihler, C. Jaeger, T. Vallaitis, M. Gjukic, M. S. Brandt, E. Pippel, J. Woltersdorf, and U. Gosele, Appl. Phys. Lett. **88**, 112506 (2006).
[5] L. Ottaviano, M. Passacantando, S. Picozzi, A. Continenza, R. Gunnella, A. Verna, G. Bihlmayer, G. Impellizzeri, and F. Priolo, Appl. Phys. Lett. **88**, 061907 (2006).
[6] S. Ahlers, D. Bougeard, N. Sircar, G. Abstreiter, A. Trampert, M. Opel, and R. Gross, Phys. Rev. B **74**, 214411 (2006).
[7] A. P. Li, C. Zeng, K. Van Benthem, M. F. Chisholm, J. Shen, S. V. S. Nageswara Rao, S. K. Dixit, L. C. Feldman, A. G. Petukhov, M. Foygel, and H. H. Weitering, Phys. Rev. B **75**, 201201 (2007).
[8] H. Li, Y. Wu, Z. Guo, P. Luo, and S. Wang, J. Appl. Phys. **100**, 103908 (2006).
[9] Y. Wang, J. Zou, Z. M. Zhao, X. H. Han, X. Y. Zhou, and K. L. Wang, Appl. Phys. Lett. **92**, 101913 (2008).
[10] X. Luo, S. B. Zhang, and S. Wei, Phys. Rev. B **70**, 033308 (2004).
[11] X. Z. Liao, J. Zou, D. Cockayne, J. Wan, Z. M. Jiang, G. Jin, and Kang L. Wang, Appl. Phys. Lett. **79**, 1258 (2001).
[12] JCPDS-ICDD Card Nos. 06-0646 ($Mn_5Ge_3$), 04-0545 (Ge), 32-0637 ($\alpha$-Mn), and 75-0589 (Si).
[13] see http://www.dayah.com/periodic/ for the atomic radius for Mn and Ge.
[14] Y. Wang, Z. M. Zeng, X. F. Han, X. G. Zhang, X. C. Sun, and Z. Zhang, Phys. Rev. B **75**, 214424 (2007).
[15] C. Y. You, A. Cerezo, P. H. Clifton, L. Folks, M. J. Carey, and A. K. Petford–Long, Appl. Phys. Lett. **91**, 011905 (2007).
[16] Y. Wang, X. L. Du, Z. X. Mei, Z. Q. Zeng, M. J. Ying, H. T. Yuan, J. F. Jia, Q. K. Xue, and Z. Zhang, Appl. Phys. Lett. **87**, 051901 (2005).
[17] C. Zeng, S. C. Erwin, L. C. Feldman, A. P. Li, R. Jin, Y. Song, J. R. Thompson, and H. H. Weitering, Appl. Phys. Lett. **83**, 5002 (2003).
[18] see http://alloy.phys.cmu.edu/ for the adhesive energies for $Mn_5Ge_3$ and a-Mn.